Organic Electronics 42 (2017) 28–33

Contents lists available at ScienceDirect

Organic Electronics

journal homepage: www.elsevier.com/locate/orgel

Quantitative estimation of exciton quenching strength at interface of charge injection layers and organic semiconductor

Aravindh Kumar [a, 1], Amrita Dey [b, 1], Anjali Dhir [c], Dinesh Kabra [b, *]

[a] Department of Electrical Engineering, Indian Institute of Technology Bombay, Powai, Mumbai, 400076, India
[b] Department of Physics, Indian Institute of Technology Bombay, Powai, Mumbai, 400076, India
[c] Department of Chemistry, Indian Institute of Technology Bombay, Powai, Mumbai, 400076, India

ARTICLE INFO

Article history:
Received 29 October 2016
Received in revised form
23 November 2016
Accepted 1 December 2016
Available online 5 December 2016

Keywords:
Exciton dynamics
Organic semiconductors
Injection layers
Dipole energy-transfer

ABSTRACT

The performance of polymer light emitting diodes (PLEDs) degrades due to exciton quenching at the interface with charge injection layers and electrodes. We investigate the photo-physics of singlet excitons in Poly (9, 9-dioctylfluorene-alt-benzothiadiazole) (F8BT) conjugated polymer interfaced with various commonly used hole and electron injection layers. Absolute, steady-state and transient photoluminescence (PL) studies are carried out on pristine F8BT film and films with injection layer/F8BT to understand the role of injection layers on exciton quenching. Exciton quenching by the charge injection layers is treated by accounting for both exciton diffusion and the non-radiative transfer of energy to the charge injection layer. The non-radiative transfer of energy is modelled using dipole-dipole interaction theory coupled with diffusion of excitons, from which we obtain the exciton capture radius (x_0) in the range of 1–7 nm. We also correlate x_0 with PL decay time (τ) using the relation $\tau \propto 1/x_0^3$. The steady-state PL yield for each case also shows correlation with the PL decay lifetime. This study provides interesting insight on the selection criterion for injection layer to be used in PLEDs for minimizing optical losses while preserving the electronic injection properties.

© 2016 Elsevier B.V. All rights reserved.

1. Introduction

Exciton generation, diffusion, recombination/dissociation are the key processes in controlling the operational performance of organic semiconductor based devices [1–3]. In these thin film devices, the charge carrier injection/collection layers and charge blocking layers play a crucial role in controlling the exciton dynamics and hence the device performance [4–7]. In order to select the right interlayer (charge injection/blocking layers) between the device electrode and active materials, one needs to look for not only the right electronic level alignment but also careful consideration of optical losses (due to various non-radiative processes) at the interfaces of interlayer/active material and metal contact/active layer are needed [2]. One of the most successful optoelectronic device based on these molecular semiconductor is organic light emitting diode (OLED). The efficiency of OLEDs is controlled mostly by the dynamics of singlet excitons [3,8,9]. Singlet exciton diffusion takes place with the help of long range Forster Resonance Energy Transfer (FRET). Different techniques have been adapted till date to study the exciton diffusion processes in molecular as well as conjugate polymer (CP) semiconductor systems [10–12]. Photoluminescence quenching method and exciton annihilation processes are some of the most popular methods to study the exciton diffusion processes [2,10]. In this study, time resolved photoluminescence quenching technique is being used to show the role of charge injection/blocking layer in F8BT PLED. We have selected the most commonly used interlayers: poly(3,4-ethylenedioxythiophene) polystyrene sulfonate (PEDOT:PSS) [13], MoO_3 [14] and ZnO [15] each of which provides a different degree of optical losses, which affects the overall device performance. A quantitative study to determine the exciton capturing strength (and hence width of the quenching region near to the electrode/interlayer/active material interface) of these injection layers can provide important insight on spatio-temporal profile of optically generated excitons. Among various active materials under the fluorescent category, polyfluorene [16] is one of the popular choices due to its bandgap tunability, chemical stability due to a deep HOMO level and semi-crystalline phases [17]. In this paper, Poly (9, 9-dioctylfluorene-alt-benzothiadiazole) (F8BT) conjugated

* Corresponding author.
E-mail address: dkabra@iitb.ac.in (D. Kabra).
[1] Authors contributed equally.

http://dx.doi.org/10.1016/j.orgel.2016.12.004
1566-1199/© 2016 Elsevier B.V. All rights reserved.

polymer interfaced with various charge injection layers (CILs) is studied in detail with the goal of understanding the role of the various injection layers on exciton dynamics of F8BT polymer system. F8BT is known to give very high photoluminescence quantum yield (η_{PLQY}~80%) and electroluminescence (EL) efficiency [7,18]. Interface dynamics of emissive layer (F8BT) and CILs play an important role on overall performance of optoelectronic devices. Due to anisotropic charge transport properties and mismatch in injection barrier of electrons and holes, most of the organic semiconductor devices have recombination zone lies close to one of the injection layer [3,7]. Hence, understanding of the role of these interfaces on fundamental levels is of great importance. We carried out steady-state photoluminescence efficiency and time resolved photoluminescence measurements on F8BT thin film with and without the charge injection layers. These results are modelled analytically using well established dipole energy transfer theory [19,20] to determine the exciton capture radii (x_0) of these injection layers and also to determine the exciton diffusion coefficient and consequently, the exciton diffusion length, in F8BT. Knowing the capture radius along with the exciton diffusion length helps in understanding polymer light-emitting-diode (PLED) device physics and can also provide design rules to improve device performance by selecting right materials combination for injection/blocking layer and emissive layer. We also demonstrate a great improvement in PLED efficiency (~2 cd/A to ~10 cd/A) to correlate the effect of interfacial quenching to real device performance.

2. Theoretical background

To model the optically generated singlet exciton formed inside the F8BT polymer layer adjacent to a CIL, we model the exciton dynamics using the one dimensional continuity equation [10],

$$\frac{\partial n(x,t)}{\partial t} = D\frac{\partial^2 n(x,t)}{\partial x^2} - r(x,t)n(x,t) + g(x,t) \tag{1}$$

The first term on the right hand side represents the diffusion term of the optically generated singlet excitons, where D is the diffusion coefficient of singlet exciton, $n(x,t)$ is the exciton concentration and $r(x,t)$ is the rate of exciton recombination which includes both radiative and non-radiative recombination pathways and $g(x,t)$ is the rate of exciton generation which depends on the spatial distribution of optical absorption of the polymer film. In our experiment, we use the Time-Correlated Single Photon Counting (TCSPC) to study the effect of CILs on the polymer film. In TCSPC technique, the decay is observed after an initial pulse (here pulse width ~ 240 ps for the present excitation wavelength of 440 nm) from the laser source. After the initial excitation, there is no further exciton generation and hence, while fitting the PL decay part, $g(x,t)$ term vanishes in Equation (1). The effect of the laser pulse is taken in the form of initial exciton distribution that is required to solve the spatio-temporal partial differential equations. The photoluminescence decay in pure F8BT obtained from TCSPC measurements is a mono-exponential decay (see Fig. S6) which allows us to account for all the exciton recombination pathways in pure F8BT using a single lifetime, which we shall call τ_0. Any possible chemical reaction of CILs with F8BT is significantly low in present study, that's why we observe mono-exponential decay in transient PL as only a single photo-physical event, i.e., non-radiative energy transfer between polymer and CILs occurs. Thus in pure F8BT our continuity equation is as follows:

$$\frac{\partial n(x,t)}{\partial t} = D\frac{\partial^2 n(x,t)}{\partial x^2} - \frac{n(x,t)}{\tau_0} \tag{2}$$

In the presence of a charge injection layer, in addition to existing radiative and non-radiative recombination pathways, we have exciton quenching at the interface with the injection layers. We have used long range dipole–dipole interaction model developed by Chance *et al* [19,20] to describe the non-radiative energy transfer between polymer and charge-injection layer. The rate of non-radiative recombination due to this energy transfer is given by:

$$r_{nr} = \frac{1}{\tau_0}\frac{x_0^3}{x^3} \tag{3}$$

where x_0 is a parameter dependent on the material properties of the polymer and the charge injection layer, which we shall call the 'capture radius' and it accounts for the effective distance of non-radiative energy transfer from polymer to the CILs. Thus, in presence of CILs, our final continuity equation has become [10]:

$$\frac{\partial n(x,t)}{\partial t} = D\frac{\partial^2 n(x,t)}{\partial x^2} - \frac{n(x,t)}{\tau_0}\left[1 + \left(\frac{x_0}{x}\right)^3\right] \tag{4}$$

Solving the parabolic partial differential Equations (2) and (3) requires the knowledge of the boundary conditions as well as the initial conditions. The initial condition, in this case, is nothing but the initial exciton profile that exists just after the optical excitation. For the boundary conditions, the derivative of exciton distribution is set to zero at both the ends, or in other words, the exciton distribution is taken to be flat at the ends. Physically, this boundary condition comes from the condition that exciton diffusion current across the interface should be zero. If the exciton distribution at the ends was anything but flat, there would be non-zero exciton diffusion current across the interface. We assume that the initial exciton distribution is proportional to the initial light intensity existing in the polymer layer when the laser pulse is beamed, since the generation of excitons is proportional to the amount of light absorbed. The initial light intensity inside the polymer layer need not be a purely exponential decay as Beer-Lambert's law might suggest because of interference due to light reflected from the polymer/air or polymer/charge injection layer interfaces. Therefore, we perform transfer-matrix calculations to obtain the profile of electric field within the polymer layer. This requires the optical constants of the interlayers and the F8BT layer which are determined by ellipsometry measurements (see in Fig. S2). The resulting light intensity distributions are calculated to find initial exciton density profile (see in Fig. S3).

3. Experimental methods

The samples for optical studies are prepared on quartz substrates and devices on ITO coated glass substrates, which are cleaned in an ultra-sonicator using soap water, DI water, acetone and IPA (2-Propanol) successively, each for 10 min. PEDOT:PSS from Sigma Aldrich is spin coated on the cleaned substrate. The spin coated PEDOT:PSS is then baked at 150 C for 30 min under constant N_2 flow. TFB layer (~10 nm) is prepared with concentration 3 g/l from p-xylene solution on top of PEDOT:PSS in N_2 filled Glove box and then annealed at 180 °C for an hour and then cooled down by placing it on a metal plate and after that the TFB coated substrate are spin rinsed with p-xylene to clear away the any remaining dissolving part. On another set of quartz substrates, MoO_3 (powder 99.999% metal basis from sigma Aldrich) film (~10 nm) is deposited using thermal evaporation integrated inside the Glove box (GB) filled with N_2 gas. For the case of TiO_2/F8BT, TiO_2 is spin coated on the cleaned quartz substrate and then annealed at 100 °C for 15 min and then 500 °C for 30 min. For TiO_2/PCBA/F8BT, after TiO_2 (~30 nm) is spin-coated and the sample is annealed, the TiO_2 coated substrate is immersed in a solution of PCBA in chlorobenzene (0.1 g/

l) for 30 min. After this, the sample is flushed thrice with chlorobenzene by spinning, in order to remove the excess PCBA. For the case of ZnO(~40 nm)/$Ba(OH)_2$, the substrate is heated to 400 °C and then ZnO is deposited by spray pyrolysis from zinc acetate dehydrate (80 mg/ml) dissolved in methanol. Further $Ba(OH)_2$ procured from Sigma Aldrich is dissolved in 2-methoxy ethanol with concentration of 5 g/l and spin coated at 4000 rpm to get thickness in the range of ~ 5nm[3]. F8BT (from CDT Pvt Ltd, U.K., M_n ~ 81K, PDI ~2.6) is spun from solution in *p*-xylene (20 g/l concentration for device and 3 mg/ml for optical studies) on top of the coated substrates separately in N_2 filled glove box and baked at 155 °C for 1 h to get a thickness of ~250 nm for device and 30 nm film for optical studies. The thicknesses of the various layers are measured using a DekTak surface profilometer. Further, optical microscope visual inspection (60X objective lens, with NA 1.4) confirms pin-hole free compact smooth film of F8BT polymer on substrate with and without CILs.

Time correlated single photo counting (TCSPC) is done in HORIBA Jobin Yvon IBH TCSPC system using a 440 nm Nano-LED laser with FWHM (full width at half maximum) of 240 ps at 1 MHz frequency with ~7ps time resolution of the channel. We have carried out absolute PL yield measurement of films using a calibrated large area photo-detector by placing film (smaller than detector area) directly on top of detector. The whole setup – the sample and the photodetector – is kept in vacuum conditions. We excite the sample using a 490 nm laser diode and the light falls on the film after passing through a chopper. In this way, we collect only the forward emission of photons. Simple calculations, which use the reflectance and absorbance of the various layers, enable us to calculate the backward emission and the light lost through waveguide modes.

PLED characterization: Current density (Keithley 2400 source measurement unit) and brightness (Keithley 2000 multimeter) versus applied voltage (Keithley 2400 sourcemeter) characteristics for the LEDs are measured in air for encapsulated devices using a calibrated reference Si photodetector (RS component). PL spectra is recorded with a multimode optical fiber (diameter = 300 μm) attached to an intensity calibrated Ocean Optics USB2000 spectrometer.

The simulation model to determine the capture radii for various injection layers and the diffusion coefficient of F8BT has been determined by solving partial differential equation as described in the Theoretical background with the appropriate boundary condition (also described in the Theoretical background section) using the MATLAB interface.

4. Results

Fig. 1(a) shows the typical bi-layer structure of the F8BT film used for the study. Samples are excited from the substrate side by 440 nm laser beam close to the F8BT absorption maxima (~470 nm). The F8BT chemical structure is also shown there. Steady state absorption and photoluminescence spectra of pristine F8BT film are shown in Fig. 1(b). Fig. 1(c) shows the schematic representation of the optically generated exciton dynamics. Excitons which are generated close to the CIL layers (quenching region width is represented by the capture radius of the quencher) decay non-radiatively whereas excitons situated far from the quenching zone decay radiatively.

We have measured photoluminescence yield for pristine F8BT, PEDOT:PSS/F8BT, MoO_3/F8BT, ZnO/$Ba(OH)_2$/F8BT. We ensure that there is no interfusion of these two layers, by hard baking underneath layer inside an inert environment. Baked PEDOT:PSS films do not dissolve in xylene solution used for F8BT polymer and other CILs are oxide based and hence are non-reactive with F8BT. More

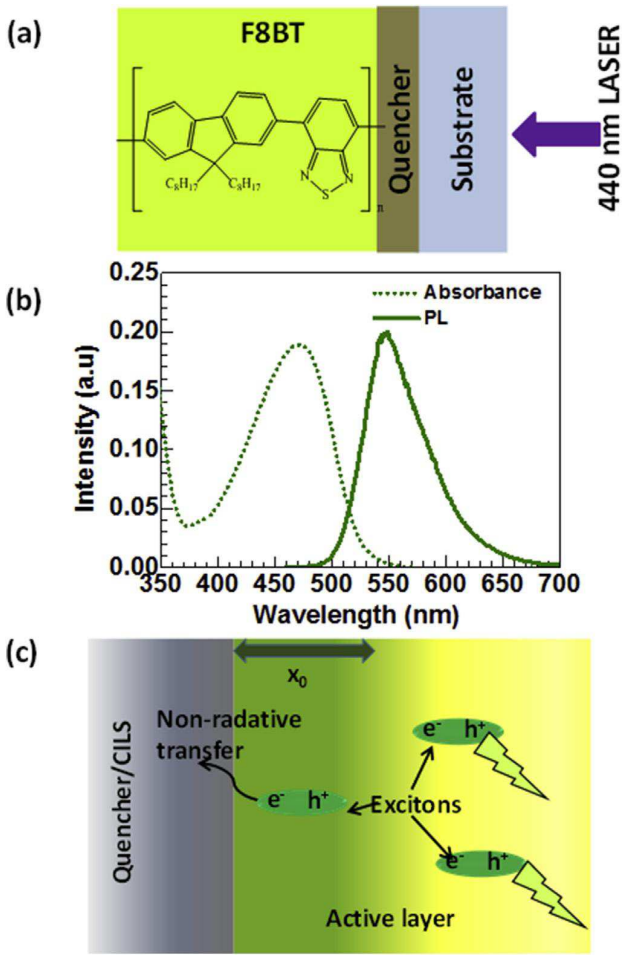

Fig. 1. (a) Bilayer structure with various injection layers/F8BT emissive layer used for studies and Chemical structures of F8BT polymer. (b) Steady-state absorbance and photoluminescence spectra of F8BT film without any CIL. (c) Schematic of different decay channels available to optically excited excitons adjacent to charge injection layers.

details discussion on it is already given in experimental section. The results of these measurements are shown in Table 1. The ratio of the decay lifetime to the PLQE (photoluminescence quantum efficiency) is found to be roughly the same in each of the four cases, which is expected according to the following Equations. If the radiative and non-radiative decay lifetimes are τ_r and τ_{nr} (the radiative and non-radiative rates being k_r and k_{nr} respectively, then using the following relations we can determine τ_r as follows [21],

$$k = k_r + k_{nr} = \frac{1}{\tau_r} + \frac{1}{\tau_{nr}};\quad \eta_{PL} = \frac{k_r}{k} = \frac{\tau}{\tau_r};\quad \tau_r = \frac{\tau}{\eta_{PL}} \tag{5}$$

This leads us to conclude that the lifetime of radiative decay in F8BT is approximately 2.57 ns, the average of these ratios.

For time resolved PL studies, we consider seven samples – pristine F8BT, MoO_3/F8BT, PEDOT:PSS/F8BT, PEDOT:PSS/TFB/F8BT, TiO_2/F8BT and TiO_2[6,6]-phenyl-C_{61}-butyric acid (PCBA)/F8BT, ZnO/$Ba(OH)_2$ (see Figs. S4–S6). The PL (excitation wavelength – 440 nm) decays have been recorded at emission wavelength maxima of F8BT i.e, 540 nm (Fig. 1(b)) for all these samples. The time resolved PL decays, after deconvolution using the instrument response function, are shown in Fig. 2 (Figs. S4 and S5 in Supporting Information

Table 1
Results from steady-state PL yield and transient PL studies. τ is the decay lifetime and PLQE stands for photoluminescence quantum efficiency.

Quencher	τ (ns)	Capture radius (nm)	PLQE (%)	τ/PLQE ratio (ns)
Intrinsic (~30 nm)	1.91	–	74	2.59
PEDOT:PSS (~40 nm)	1.56	2.54	62	2.52
PEDOT:PSS/TFB(~10 nm)	1.85	1.48	67	2.76
MoO_3 (~10 nm)	1.39	4.48	55	2.52
ZnO(~40 nm)/$Ba(OH)_2$(~5 nm)	1.26	7.34	48	2.62

(SI)). The resulting decay lifetimes are presented in Table 1 and Table S1 (in SI). All the decays are mono-exponential in nature (see Figs. S4b and S6), thereby suggesting the existence of only one type of radiating species and that the effective range of the exciton quenching by charge injection layers (augmented by exciton diffusion) is less than the film thickness. These data and calculations suggest that ZnO/$Ba(OH)_2$ is the strongest quencher, followed by MoO_3 among all interlayer materials used in this study (see Fig. S7).

By fitting these deconvoluted decays using our model described above for non-radiative energy transfer and exciton diffusion, we were able to obtain the capture radii for ZnO/$Ba(OH)_2$, MoO_3,PEDOT:PSS, PEDOT:PSS/Poly[(9,9-dioctylfluorenyl-2,7-diyl)-co-(4,4′-(*N*-(4-sec-butylphenyl)diphenylamine)] (TFB), TiO_2 and TiO_2/PCBA layer (see Table S1) injection layers. These capture radii can be used as a thumb rule when designing PLEDs (Polymer light emitting diode). The quencher, which is the injection layer here, is able to significantly influence the exciton lifetime which are within distance $L_{eff} = x_0 + L_d$, away from the interface, where x_0 is the capture radius and L_d is the exciton diffusion length in F8BT. Therefore L_{eff} represents the effective distance for non-radiative energy transfer. Thus it is desirable to have the recombination zone in case of PLEDs to lie outside this range to improve the efficiencies. Inclusion of the spacer layer between the emissive layer and the quenching interface enhance the efficiency of the devices in great extent by reducing the non-radiative quenching from the interfacial layers. As we have shown here introduction of an ultrathin layer (~10 nm) of TFB introduced as spacer layer reduces the non-radiative energy transfer which has been reflected in a five times enhancement in the current efficiency in F8BT PLED (Fig. 3**(b)**). Introduction of TFB between PEDOT:PSS and F8BT layers reduces the capture radius from 2.54 nm (PEDOT:PSS/F8BT) to 1.48 nm (PEDOT:PSS/TFB/F8BT) (see Table 1). This reduction of non-radiative energy transfer distance is clearly being reflected in the PLED performance (Fig. 3**(a)** and **(b)**). Diffusion coefficient (D) of F8BT is estimated by using Equation (2) and Equation (4) after fitting the time resolved PL data. The diffusion coefficient for F8BT is determined from fitting of PL decay in pristine F8BT using our model, and this fit is shown in Fig. 2(a). The gives us D (singlet exciton diffusion coefficient) ~ 2×10^{-4} cm^2s^{-1} in F8BT polymer system which agrees well with the value reported in literature [22]. The diffusion length in F8BT, which can be calculated from the radiative lifetime and diffusion coefficient of F8BT, comes out to be 8.09 nm [2]. Fig. 4**(a)** shows both spatial and temporal variation of exciton concentration in MoO_3/F8BT system (Fig. S1 shows in SI, the same for PEDOT:PSS/F8BT, ZnO/$Ba(OH)_2$/F8BT interfaces). From this data at time ~0.2 ns, we get the spatial exciton profile at 0.2 ns after the laser pulse, which is shown in Fig. 4**(b)**. The maximum exciton concentration is found at around 11.5 nm away from the quencher with the concentration falling on either side due to non-radiative energy transfer to the quencher on one side and the lack of photo excitation, due to a decrease in the amount of light absorbed, on the other side. Shown in Fig. 4**(c)** is the temporal exciton profile at 20 nm away from the quencher in MoO_3. Knowing the diffusion length and the capture radius in MoO_3, we can say that the quenching influence of the charge injection layer is significant as

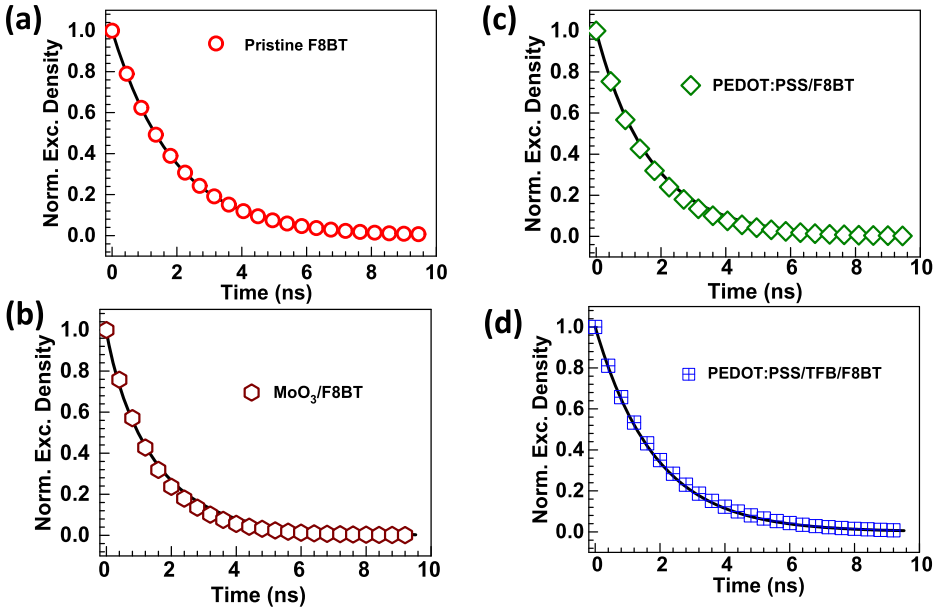

Fig. 2. Normalized exciton density decay profile with respect to time for (a) pristine F8BT, (b) MoO_3/F8BT, (c) PEDOT:PSS/F8BT and (d) PEDOT:PSS/TFB/F8BT. Solid lines show the fit (see Equation (5)) to experimental data.

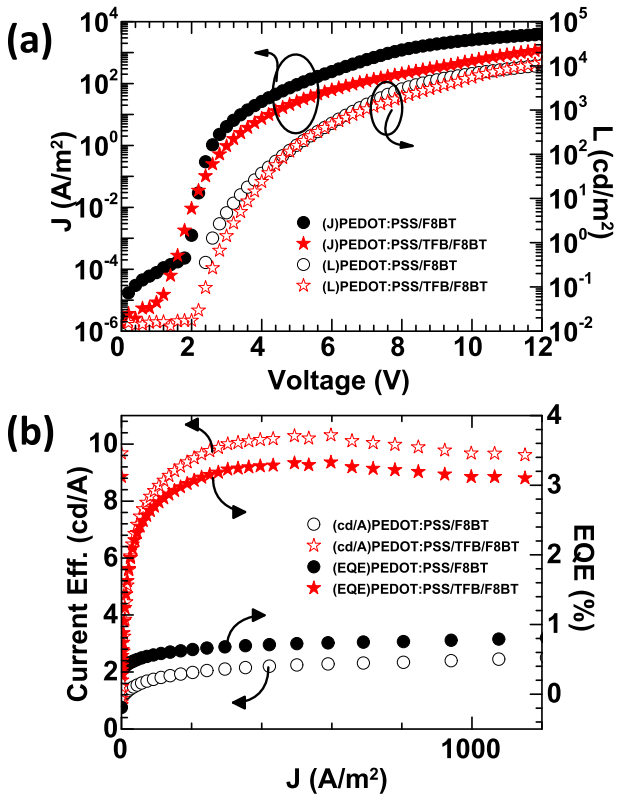

Fig. 3. **(a)** Current (solid) -Voltage-Luminance (hollow) characteristics and **(b)** current efficiency (cd/A) & External quantum efficiency (EQE) vs injection current for ITO/PEDOT:PSS/F8BT/Ca/Al (black ○) and ITO/PEDOT:PSS/TFB (~5 nm)/F8BT/Ca/Al (red ☆) structures. (For interpretation of the references to colour in this figure legend, the reader is referred to the web version of this article.)

far as ~11.8 nm away from the interface. We plotted the capture radii vs lifetime for each the following charge injection layers along with spacer layer - PEDOT:PSS, PEDOT:PSS/TFB, MoO_3, ZnO/$Ba(OH)_2$, TiO_2 and TiO_2/PCBA, which is shown in Fig. 4**(d)**, and found that the plot can be fitted very well by the relation $\tau \propto 1/x_0^3$.

5. Discussions

Emissive layer which is in contact with the metal or metal oxide interface loses its energy via non radiative energy transfer from excited polymer layer to the metallic interface via long range dipole interaction. The rate of non-radiative energy transfer follows an inverse cube law (as described in the theoretical model) with distance from the interface. The most quenching interface is ZnO/$Ba(OH)_2$/F8BT with capture radius ~7.34 nm followed by MoO3/F8BT where the capture radius is ~4.47 nm. Reason for finding higher quenching strength of MoO_3 and ZnO/$Ba(OH)_2$ layers might be due to interfacial doping of F8BT [6,23,24].

Introduction of an ultrathin spacer layer between metallic interface and the emissive layer modifies the non-radiative energy transfer (equation (3)) by

$$r_{nr} = \frac{1}{\tau_0}\frac{x_0^3}{(x+d)^3}$$

where d is the space layer thickness. This enhances the lifetime of the excited species and improves the device efficiency. TFB is used as a spacer layer between PEDOT:PSS/F8BT interface in polymer light emitting diodes. Transient PL of F8BT showed an evident enhancement in decay time (see Fig. 2(d)), which is again modelled to determine capture radii (x_0) (see Table 1). As expected we found a reduction in x_0 from 2.54 nm for PEDOT:PSS/F8BT interface to 1.48 nm for PEDOT:PSS/TFB/F8BT interface. Further, PLEDs are fabricated using ITO/PEDOT:PSS/Spacer-layer/F8BT/Ca/Al structure.

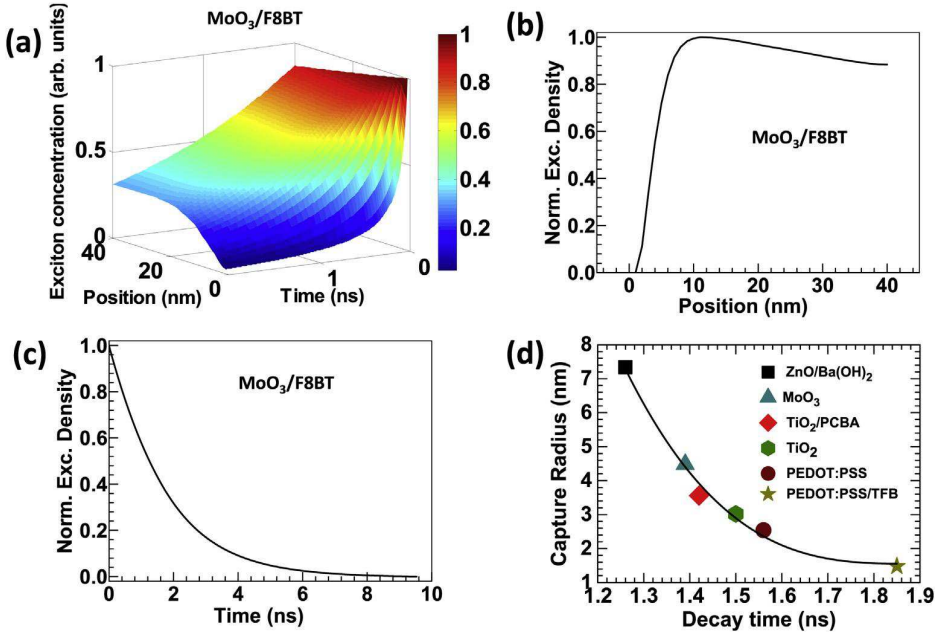

Fig. 4. **(a)** Simulated normalized spatio-temporal profile of exciton density inside F8BT layer with MoO3 as injection layer. Normalized exciton density profile **(b)** with respect to distance from MoO3 injection layer at t = 0.2ns and **(c)** with respect to time at 20 nm away from MoO3 injection layer inside F8BT polymer film. **(d)** Plot of capture radii determined from the model vs the decay lifetime for all CILs (including MoO3/F8BT, PEDOT:PSS/F8BT,PEDOT:PSS/TFB/F8BT, TiO_2/F8BT, TiO_2/PCBA/F8BT) with a curve fit of the form $y = a\,x^{-3} + b$.

The device efficiency enhances (see[19] Fig. 4) from ~2.5 cd/A to ~10.4 cd/A by reducing the non-radiative quenching of the emissive singlet exciton at the PEDOT:PSS/F8BT interface by moving the recombination zone away (TFB interlayer thickness ~ 10 nm) from the PEDOT:PSS interface. We acknowledge that further improvement can be made by selecting optimal thickness of TFB interlayer. However, focus of this manuscript is to understand the exciton capture strength of commonly used injection layers for PLEDs. We used multiple injection layers instead of optimizing a single interlayer where one would not only need to understand photo-physics but also charge transport properties and photonics of used device structure needs to be studied and optimized [10,25].

6. Conclusions

In summary, we have studied exciton diffusion in F8BT and the non-radiative energy transfer across the interface with commonly used charge injection layers. The knowledge of steady state PL yield along with transient PL decay allows us to disentangle the non-radiative and radiative channels of exciton decay and the radiative decay lifetime is determined to be ~2.57 ns. Using transient PL measurements in pristine F8BT, we determine the diffusion coefficient (~2×10^{-4} cm^2s^{-1}). The knowledge of the radiative decay lifetime and the diffusion coefficient allows us to calculate the exciton diffusion length (L_d) which comes out to be ~8 nm. Finally, we have modelled the transient PL decay using a model of exciton diffusion and non-radiative energy transfer that allows us to quantify the PL quenching strength of CILs in terms of exciton capture radius (x_0). Our studies also provide photo-generated exciton concentration spatial profile and its evolution with time in the F8BT active layer. Quantifying exciton capture strength provides insight when inserting transport layers or spacer layers in between electrode and emissive layer to suppress quenching in order to minimize optical losses while preserving the injection properties of holes is also demonstrated using insertion of TFB interlayer in between PEDOT:PSS/F8BT interface.

Acknowledgements

We thank Cambridge Display Technology (CDT), Ltd., for supplying F8BT. This work is partially supported by the IITB Seed grant (12IRCCSG044) and DST-India (SB/S3/ME/037/2014). We also acknowledge support of Centre of Excellence in Nanoelectronics (CEN) for device fabrication facility. AD acknowledges UGC for research fellowship.

Appendix A. Supplementary data

Supplementary data related to this article can be found at http://dx.doi.org/10.1016/j.orgel.2016.12.004.

References

[1] D. Markov, P. Blom, Exciton quenching in poly (phenylene vinylene) polymer light-emitting diodes, Appl. Phys. Lett. 87 (2005) 233511.
[2] Y. Tamai, H. Ohkita, H. Benten, S. Ito, Exciton diffusion in conjugated polymers: from fundamental understanding to improvement in photovoltaic conversion efficiency, J. Phys. Chem. Lett. 6 (2015) 3417–3428.
[3] A. Dey, A. Rao, D. Kabra, A complete quantitative analysis of spatio-temporal dynamics of excitons in functional organic light-emitting diodes, Adv. Opt. Mater. (2016), http://dx.doi.org/10.1002/adom.201600678.
[4] J.S. Park, B.R. Lee, J.M. Lee, J.-S. Kim, S.O. Kim, M.H. Song, Efficient hybrid organic-inorganic light emitting diodes with self-assembled dipole molecule deposited metal oxides, Appl. Phys. Lett. 96 (2010) 243306.
[5] J.-S. Kim, R.H. Friend, I. Grizzi, J.H. Burroughes, Spin-cast thin semiconducting polymer interlayer for improving device efficiency of polymer light-emitting diodes, Appl. Phys. Lett. 87 (2005) 023506.
[6] L.P. Lu, D. Kabra, R.H. Friend, Barium hydroxide as an interlayer between zinc oxide and a luminescent conjugated polymer for light-emitting diodes, Adv. Funct. Mater. 22 (2012) 4165–4171.
[7] D. Kabra, L.P. Lu, M.H. Song, H.J. Snaith, R.H. Friend, Efficient single-layer polymer light-emitting diodes, Adv. Mater. 22 (2010) 3194–3198.
[8] N.C. Giebink, S.R. Forrest, Quantum efficiency roll-off at high brightness in fluorescent and phosphorescent organic light emitting diodes, Phys. Rev. B 77 (2008) 235215.
[9] A. Monkman, Singlet generation from triplet excitons in fluorescent organic light-emitting diodes, ISRN Mater. Sci. 2013 (2013).
[10] D.E. Markov, Excitonic Processes in Polymer-based Optoelectronic Devices, University Library Groningen, 2006. Host.
[11] S. Hofmann, T.C. Rosenow, M.C. Gather, B. Lüssem, K. Leo, Singlet exciton diffusion length in organic light-emitting diodes, Phys. Rev. B 85 (2012) 245209.
[12] D. Kabra, K. Narayan, Direct estimate of transport length scales in semiconducting polymers, Adv. Mater. 19 (2007) 1465–1470.
[13] K. Murata, S. Cina, N. Greenham, Barriers to electron extraction in polymer light-emitting diodes, Appl. Phys. Lett. 79 (2001) 1193–1195.
[14] K. Reynolds, J. Barker, N. Greenham, R. Friend, G. Frey, Inorganic solution-processed hole-injecting and electron-blocking layers in polymer light-emitting diodes, J. Appl. Phys. 92 (2002) 7556–7563.
[15] Y. Vaynzof, D. Kabra, L. Zhao, P.K. Ho, A.T.-S. Wee, R.H. Friend, Improved photoinduced charge carriers separation in organic-inorganic hybrid photovoltaic devices, Appl. Phys. Lett. 97 (2010) 033309.
[16] Y. Zhang, P.W. Blom, Electron and hole transport in poly (fluorene-benzothiadiazole), Appl. Phys. Lett. 98 (2011) 143504.
[17] C.L. Donley, J. Zaumseil, J.W. Andreasen, M.M. Nielsen, H. Sirringhaus, R.H. Friend, J.-S. Kim, Effects of Packing Structure on the Optoelectronic and Charge Transport Properties in Poly(9,9-di-n-octylfluorene-alt-benzothiadiazole), J. Am. Chem. Soc. 127 (2005) 12890–12899.
[18] M. Sessolo, H.J. Bolink, Hybrid organic–inorganic light-emitting diodes, Adv. Mater. 23 (2011) 1829–1845.
[19] R. Chance, A. Prock, R. Silbey, Lifetime of an emitting molecule near a partially reflecting surface, J. Chem. Phys. 60 (1974) 2744–2748.
[20] R. Chance, A. Prock, R. Silbey, Comments on the classical theory of energy transfer, J. Chem. Phys. 62 (1975) 2245–2253.
[21] S. Strickler, R.A. Berg, Relationship between absorption intensity and fluorescence lifetime of molecules, J. Chem. Phys. 37 (1962) 814–822.
[22] M.A. Stevens, C. Silva, D.M. Russell, R.H. Friend, Exciton dissociation mechanisms in the polymeric semiconductors poly (9, 9-dioctylfluorene) and poly (9, 9-dioctylfluorene-co-benzothiadiazole), Phys. Rev. B 63 (2001) 165213.
[23] M.C. Gwinner, R.D. Pietro, Y. Vaynzof, K.J. Greenberg, P.K. Ho, R.H. Friend, H. Sirringhaus, Doping of organic semiconductors using molybdenum trioxide: a quantitative time-dependent electrical and spectroscopic study, Adv. Funct. Mater. 21 (2011) 1432–1441.
[24] Y. Vaynzof, D. Kabra, L.L. Chua, R.H. Friend, Improved electron injection in poly(9,9′-dioctylfluorene)- co-benzothiodiazole via cesium carbonate by means of coannealing, Appl. Phys. Lett. 98 (2011) 113306.
[25] J. Bailey, E.N. Wright, X. Wang, A.B. Walker, D.D. Bradley, J.-S. Kim, Understanding the role of ultra-thin polymeric interlayers in improving efficiency of polymer light emitting diodes, J. Appl. Phys. 115 (2014) 204508.